THE REGION OF TRIGGERED STAR FORMATION W40: OBSERVATIONS AND MODEL

L. E. Pirogov[1,2,*]

[1] *Institute of Applied Physics Russian Academy of Sciences, Nizhni Novgorod, Russia*

[2] *Lobachevsky State University of Nizhni Novgorod, Nizhni Novgorod, Russia*

A "collect and collapse" model of triggered star formation is used to estimate the parameters of ring-like structure consisted of a sequence of low-mass clumps in the W40 region. The model parameters are close to the observed ones if the density of the cloud in which the HII zone is expanding is fairly high ($\gtrsim 10^5$ cm^{-3}) and the luminosity of the driving source exceeds previous estimate. Probable reasons for the scatter of the observed parameters of the clumps are discussed.

1. INTRODUCTION

Early stages of the star formation process are far from fully understood in spite of increasing amount of observational data available. This is true, in particular, for regions of high-mass star formation which are more rare, more distant, and evolve more quickly than regions of low-mass star formation, spend considerable time of their evolution inside the parent cloud (e.g. [1]). As massive stars evolve, they affect parent cloud through their stellar winds, massive outflows, strong UV-radiation, and expansion of their HII zones. These factors change the physical conditions and chemical composition of the cloud and the expanding of HII zones "sweep out" the gas towards the periphery causing compression and possibly trigger the formation of a new generation of stars.

The W40 region (Sharpless 64) [2, 3] contains large blister-type HII zone that lies at the edge of an extended molecular cloud (TGU 279-P7 [4]) in the Aquila Rift complex. According to recent estimates the distance to the central sources of the HII zone is ~ 500 pc [5]. This puts W40 among the nearest regions of high-mass star formation. The difference between CO and hydrogen recombination line velocities indicates that the HII zone lies at the front

* Electronic address: pirogov@appl.sci-nnov.ru

edge of the cloud closer to the observer [6]. The HII region expands into molecular cloud to the west. Molecular gas is observed is observed at two different velocities which probably correspond to gas located behind and in front of the HII zone [7]. The W40 region was studied at various wavelengths from the radio to the X-ray (see the review [8] and [5, 9–13]).

Continuum observations of dust emission [11, 12] have shown that the dust to the west of the HII zone is concentrated in clumps forming a ring. The morphology of ionized gas [12, 13] shows that there is another compact HII zone near the main one. The expansion of this zone could lead to formation of the ring-like structure due to the "collect and collapse" mechanism. This model was proposed in [14] to describe the process of triggered high-mass star formation. Although there are more than a few examples where this mechanism could be taking place (e.g. [15–19]) there have been few quantitative comparisons between observational data and the model. This can be related to the fact that the model is fairly simple compared to real objects with inhomogeneous density structure. In the W40 region which is located much more closer than most of the HII zones where the collect and collapse mechanism could take place the observed ring-like structure is more distinct and compact and is much closer to the probable driving source of the HII region. We present here quantitative comparison of the physical parameters derived from observations with the model predictions in order to determine whether the collect and collapse model can predict parameters of the structure found in W40.

2. THE RING OF DUST CLUMPS

A 1.2 mm dust continuum emission map of W40 taken from [12] is given in the figure. The dust is concentrated in a chain of clumps forming a ring. The data of [11] show that the western branch of the ring extends to the northeast, making the ring-like structure more distinct. Some of the clumps are associated with the Class 0 and Class I sources [11], indicating that low-mass star formation has started in the ring. The Near-IR sources [5] and 3.6 cm compact VLA radio sources [9] are also shown in the figure (left panel).

Most of the radio and IR sources are grouped near the driving source of the main HII zone (IRS 1A South), which is located to the east of the ring and appears to be a massive O9.5 star [5, 13]. The IRS 5 infrared source, which is a B1 star and the probable source of the neighboring compact HII zone [12, 13], is also marked in the figure. Since IRS 5 is located

within the region bounded by the ring, but is shifted relative to its geometrical center, it is probable that the ring formed due to the expansion of the compact zone around this source. The ring is apparently not oriented face-on, and its south-eastern part is closer to observer [12].

The formation of the ring-like structure from a sequence of fragments (clumps) suggests the action of collect and collapse mechanism of triggered star formation [14]. This mechanism is treated analytically in [20] and the results of that paper have been confirmed by model calculations [21]. According to the collect and collapse mechanism when an HII region expands into molecular cloud, a layer of enhanced density forms between the shock front and the ionization front. Due to instability, the layer splits into uniformly spaced clumps, which can be the sites of formation of next generation of stars. Such ring-like structures usually consisting of massive fragments ($M \sim 10 - 100\ M_\odot$) are observed at the edges of some HII zones (e.g. [15, 16, 18]). However, in the case of W40, the masses of clumps in the ring ($0.4 - 8\ M_\odot$ [12]) are considerably lower than is usually observed in such structures.

3. ANALYTICAL MODEL

The evolution of the layer formed while an HII zone expands into a medium consisted of neutral gas with uniform density is considered in [20]. Analytical expressions for the time at which fragmentation in the layer occurs (t_{frag}), the layer radius (R_{frag}) and column density of the layer (N_{frag}) at this time, the mean mass of fragments (M_{frag}) and initial separation between fragments ($2r_{frag}$) have been derived. They depend on the sound speed in the medium (a), on the density of atomic gas (n), and on the luminosity of the central source of ionized radiation (L). The expressions of [20] are given below, where $a_{0.2} = a/0.2\,\mathrm{km/s}$, $L_{49} = L/10^{49}\,\mathrm{photon/s}$, $n_3 = n/10^3\,\mathrm{cm}^{-3}$:

$$t_{frag} \sim 1.6\,\mathrm{Myr}\ \ a_{0.2}^{7/11} L_{49}^{-1/11} n_3^{-5/11}\ , \tag{1}$$

$$R_{frag} \sim 5.8\,\mathrm{pc}\ \ a_{0.2}^{4/11} L_{49}^{1/11} n_3^{-6/11}\ , \tag{2}$$

$$N_{frag} \sim 6 \times 10^{21}\,\mathrm{cm}^{-2}\ \ a_{0.2}^{4/11} L_{49}^{1/11} n_3^{5/11}\ , \tag{3}$$

$$M_{frag} \sim 23\, M_\odot \;\; a_{0.2}^{40/11} L_{49}^{-1/11} n_3^{-5/11} \;, \tag{4}$$

$$2r_{frag} \sim 0.8\,\mathrm{pc} \;\; a_{0.2}^{18/11} L_{49}^{-1/11} n_3^{-5/11} \;. \tag{5}$$

Note that, when the gas is in molecular form, the atomic gas density is twice of the molecular gas density [21]. We neglected this factor in our approximate estimates derived from (1)–(5).

It is clear from the above equations that, when the HII zone made by a star emitting 10^{49} photons/s (main sequence O6 massive star [22]) expands into a cold cloud with moderate density ($T_{\rm KIN} \sim 10 - 15$ K, $n \sim 10^3$ cm^{-3}), a layer of fragments with masses $\sim 25 - 40\ M_\odot$ forms at a distance ~ 6 pc after ~ 1.6 Myr. The initial separation between centers of the fragments is ~ 1 pc. Such fragments could become sites of formation of a new generation of stars, including massive ones. If an HII zone expands into a medium of higher density, the layer of enhanced density will form on shorter scales and closer to the star. This layer will split into fragments with lower sizes and masses.

The luminosity of IRS 5, the source that has probably formed the ring-like structure in W40, is $\sim 2.4 \times 10^{45}$ photons/s, which corresponds to a B1V star [13]. IRS 5 is classified as a B1 star in [5]. However, the luminosity could be appreciably underestimated, as well as the luminosity of the main HII zone (see the discussion in [13]). We used two luminosities in calculations: one close to the estimate of [13] and the second an order of magnitude higher. The results of comparing the model calculations data with the observed parameters are given in the following section.

4. COMPARISON OF THE MODEL AND THE OBSERVED CLUMP PARAMETERS

The dense core of the molecular cloud near the HII zone in W40 has a structure consisting of several components, including clumpy ring and gas which that has not condensed into clumps [12]. The western clumps *6–9* are associated with the N_2H^+ and NH_3 molecular line emission regions, while the CS emission is enhanced towards the eastern clumps *1–3* (Figure, right panel). THe mean densities in clumps derived from continuum observations are: $\sim 10^5 - 10^6$ cm^{-3}, while the densities calculated from molecular line data are higher. The gas densities of extended regions that do not correlate with the ring and are observed

mainly in the HCO^+(1–0) and HCN(1–0) lines (Figure, right panel) should be also fairly high (the critical densities for the excitation these transitions are $\sim 10^5 - 10^6$ cm^{-3}). The ratios of the HCN(1–0) hyperfine components imply moderate optical depth [12]. The HCN(1–0) emission is apparently associated with regions of high density and not with enhanced column density of the gas. The spatial distributions of the different CO isotopic line intensities [23] correlate weakly with the ring structure, and may be tracers of a more diffuse envelope around the ring. The clumpy ring probably formed due to the expansion of the HII zone associated with IRS 5 into the parent dense cloud. In this case the gas emitting in the HCO^+ and HCN lines may represent material that has not experienced the expansion of the HII zone, since it is more distant from the source.

The Table presents parameters calculated from (1)–(5) for $a_{0.2} \approx 1.15$ ($T_{\rm KIN}$ = 15 K, $m = 2.33\ m_H$) and for two luminosities, one close to the estimate of [13] and the other an order of magnitude higher. The density of the surrounding medium for which the model estimates are more or less close to the observed parameters is given for each luminosity. The kinetic temperature value was taken to be close to kinetic and/or dust temperature estimates for the western clumps [11, 12]. The eastern clumps *1–3* associated with Class I sources [11] have higher dust temperatures, and are influenced by the ionization front of the main HII zone, which probably changes their physical characteristics. The ranges of physical parameters obtained from the observations [12] are given in the table for comparison. The parameters of the eastern clumps *1–3* are excluded from consideration.

The size of the H II zone around IRS 5 has been approximately estimated in [13] as the diameter of the ring of Class 0/I sources, $\sim$ 0.4 pc. However, this ring is probably not oriented face-on, with its eastern part is closer to the observer and different distances from the probable central source IRS 5 to the boundary of the ring in different directions (see Figure). The maximum distance between IRS 5 and the inner boundary of the ring in the southern direction is $\sim$ 0.4 pc [12], which is twice the radius estimated in [13]. The average of these two radius estimates, 0.3 pc, is given in the table as an observed radius of the ring, R_{frag}.

To be compared with the time at which gas in the layer becomes gravitationally unstable and splits into fragments (t_{frag}), the corresponding dynamical age of the HII zone (t_{dyn}) is given in the table. This was calculated from the standard expression for the time dependence of the radius of an H II zone [24] for a given luminosity and density: $R(t) = R_s(1 + \frac{7\,c_{II}\,t}{4\,R_s})^{4/7}$,

where R_s is the radius of the Strömgren zone which depends on the source luminosity and the density of the medium (e.g. [13]), and c_{II} is the sound speed of the ionized gas, taken to be 11 km/s [13]. The condition $t_{dyn} \gtrsim t_{frag}$ is satisfied in the calculations.

The ranges of the peak column densities and masses calculated from the dust continuum observations are given in the table as the observed values of N_{frag} and M_{frag}. The standard gas-to-dust mass ratio, equal to 100 [12] was adopted. Variations of these values are more likely related to density variations in the gas into which the HII zone is expanding. Variations of the gas-to-dust mass ratio in clumps (Section 5) could also be a possible reason. The observed separations between fragments ($2r_{frag}$) lie in the range indicated in the table due to probable density variations and projection effects. It is possible that the separations between the western clumps *7, 8* and *9* depend on these factors to a lesser extent. The observed clump sizes (0.02–0.11 pc) and masses are typical for low-mass star forming regions, but there are several indications that the formation of stars with masses higher than a solar mass is occurring in the eastern part of the ring [12].

A comparison between the observed parameters of the clumpy ring and the two sets of model parameters (see the table) shows that the model with higher luminosity fits the observations better. According to the model estimates, in both cases, the density of the medium into which the HII zone expands considerably exceeds the value usually adopted as a standard for neutral gas surrounding HII zones ($\sim 10^3$ см$^{-3}$). A better agreement between the model estimates of the masses and the separations of the fragmetns can be achieved if a lower temperature is adopted for the medium ($\sim$ 10 K). The density of the medium is not appreciably changed in this case. The small excess of the observed radius and column density of the layer over the model estimates (see the table) could be connected with the evolution of these parameters during the time that has passed since the onset of fragmentation in the layer.

5. DISCUSSION

The structure of the W40 dense core probably formed due to the influence on the neutral material of two HII zones whose main driving sources are IRS 1A South and IRS 5 (Figure, left panel). There is a cluster of sources near IRS 1A South. Two of these sources (IRS 2B, IRS 3A) are massive B4 and B3 stars, respectively [5]. The main H II region to the west

is bounded by dense molecular gas and is more extended in the eastern direction [13]. Its emission overlaps with emission of several compact H II zones (the figure, left panel; Fig. 10 from [13]). The HII zone around IRS 5 is located to the northwest from the main zone, has a more or less circular morphology, and is probably a distinct region. The morphology of the ionized gas shows that, even taking into account possible projection effects, it is not possible to explain the formation of the ring due to the influence of the main HII zone, since its main driving source, IRS 1A, is located to the east of the ring. Alternative mechanisms for triggered star formation such as, radiation-driven implosion, are unlikely be able to explain the formation of the observed ring-like structure with regularly spaced clumps.

As model calculations show (e.g. [25]) radiation-driven implosion can form globules of elongated (cometary or pillar-like) form that are associated with already existing inhomogeneities in the medium. Star formation occurs at their front edges (facing the star). Moreover, this mechanism predicts the existence of velocity gradients inside the globules [26], which are not observed in the clumps forming the ring-like structure in W40. Nevertheless, radiation-driven implosion could take place at the outer boundary of the eastern branch of the ring, where the morphologies of the ionized gas (according to observations with high spatial resolution), dust and dense molecular gas are similar. The line-of-sight velocities of the gas associated with the eastern clumps differ from the velocities of the remaining gas in the region, and this gas is contracting [12]. Therefore, the collect and collapse mechanism seems to be the most probable reason for the formation of the ring if the luminosity of IRS 5 is higher than the estimate of [13] and the medium where ionization front propagates has a high density.

The observed scatter of the clump masses, column densities, and separation could be associated with density variations in the medium around IRS 5. The scatter in the clump separations could be connected with both density variations and projection effects.

Note that clump masses and column densities were calculated in [12] using dust continuum observations. The gas-to-dust mass ratio was taken to be 100. It cannot be ruled out that this ratio could vary in the dense gas near an HII zone. For example, the HCN, HCO^+, CS and ^{13}CO molecular emission is detected inside the region bounded by the ring, where the dust emission is considerably reduced [11, 12, 23]. It is shown in [27] that spatial fluctuations of the dust density in turbulent clouds can occur independently of gas-density fluctuations on scales compared with the sizes of protostellar cores.

It is possible the level of turbulence of the medium increases as shock propagates, leading to spatial fluctuations in the gas-to-dust abundance ratio. The observations show that the widths of the N_2H^+, NH_3 and $H^{13}CO^+$ lines associated with the western clumps are half the widths of the CS, HCN and HCO^+ lines [12]. In addition to the optical depth effects this could be related with different levels of turbulence in the gas that emits effectively in these lines. Thus, it is possible that the gas with higher level of turbulence emitting in the CS, HCN and HCO^+ lines and spatially uncorrelated with the clumps could have a lower dust abundance. The hypothesis that there may be a relation between turbulence and spatial fluctuations of dust abundance close to HII zones need to be studied further, using both independent observational estimates of gas and dust abundances and model calculations.

6. CONCLUSION

We have carried out a comparison of the observed parameters of a ring-like structure consisting of low-mass clumps in W40 and estimates produced using the collect and collapse model [14, 20]. The physical parameters of the clumps were taken from [12]. This comparison shows that parameters such as the radius of the ring, the masses and gas column densities in the clumps, and the separation between clumps are close to the model estimates if the density of the cloud into which the HII zone expands is fairly high ($\gtrsim 10^5$ см$^{-3}$) and the luminosity of the source driving the HII zone exceeds the previous estimate [13]. Thus, W40 can be considered an example of the realization of the collect and collapse mechanism at a relatively small distance from the source in a high-density medium. The observed scatter of the physical parameters of the clumps could be associated with density inhomogeneities in the medium where ionization front propagates, and also with projection effects and turbulence of the medium that results in fluctuations of the gas-to-dust mass ratio.

ACKNOWLEDGMENTS

We thank D. Z. Wiebe for his question concerning quantitative estimates of the parameters of the collect and collapse model for W40 which inspired this study. We also thank the referee for valuable comments and questions that led to recalculation of the model parameters and a significant makeover of the paper. This work was partially supported by

Russian Foundation for Basic Research (grants 12-02-00861, 13-02-92697, 13-02-12220) and the grant (the agreement of August 27, 2013 No. 02.B.49.21.0003 between The Ministry of education and science of the Russian Federation and Lobachevsky State University of Nizhni Novgorod).

---

1. H. Zinnecker and H. W. Yorke, Ann. Rev. Astron. and Astrophys. **45**, 481 (2007)
2. S. Sharpless, Astrophys. J. Suppl. **4**, 257 (1959)
3. G. Westerhout, Bull. Astron. Inst. Netherlands **14**, 215 (1958)
4. K. Dobashi, H. Uehara, R. Kandori, T. Sakurai, M. Kaiden, T. Umemoto, F. Sato, Publ. Astron. Soc. Jap. **57**, S1 (2005)
5. R. Y. Shuping, W. D. Vacca, M. Kassis and K. C. Yu, Astron. J. **144**, 116 (2012)
6. M. Zeilik and C. J. Lada, Astrophys. J. **222**, 896 (1978)
7. J. P. Vallée, Astron. and Astrophys. **178**, 237 (1987)
8. S. A. Rodney and B. Reipurth, Handbook of Star Forming Regions **II**, 683 (2008)
9. L. F. Rodríguez, S. A. Rodney, B. Reipurth, Astron. J. **140**, 968 (2010)
10. M. A. Kuhn, K. V. Getman, E. D. Feigelson, B. Reipurth, S. A. Rodney, G. P. Garmire, Astrophys. J. **725**, 2485 (2010)
11. A. J. Maury, P. André, A. Men'shchikov, V. Könyves, S. Bontemps, Astron. and Astrophys. **535**, A77 (2011)
12. L. Pirogov, D. K. Ojha, M. Thomasson, Y.-F. Wu, I. Zinchenko, Mon. Not. RAS **436**, 3186 (2013)
13. K. K. Mallick, M. S. N. Kumar, D. K. Ojha, R. Bachiller, M. R. Samal, L. Pirogov, Astrophys. J. **779**, 113 (2013)
14. B. G. Elmegreen and C. J. Lada, Astrophys. J. **214**, 725 (1977)
15. L. Deharveng, B. Lefloch, A. Zavagno, J. Caplan, A. P. Whitworth, D. Nadeau, S. Martín, Astron. and Astrophys. **408**, L25 (2003)
16. L. Deharveng, B. Lefloch, S. Kurtz, D. Nadeau, M. Pomarès, J. Caplan, A. Zavagno, Astron. and Astrophys. **482**, 585 (2008)
17. L. Deharveng, F. Schuller, L. D. Anderson, A. Zavagno, F. Wyrowski, K. M. Menten, L. Bronfman, L. Testi, C. M. Walmsley, M. Wienen, Astron. and Astrophys. **523**, A6 (2010)

18. H. Ohlendorf, T. Preibisch, B. Gaczkowski, T. Ratzka, J. Ngoumou, V. Roccatagliata, R. Grellmann, Astron. and Astrophys. **552**, A14 (2013)
19. M. R. Samal, A. Zavagno, L. Deharveng, S. Molinari, D. K. Ojha, D. Paradis, J. Tigél, A. K. Pandey, D. Russeil, Astron. and Astrophys. **566**, A122 (2014)
20. A. P. Whitworth, A. S. Bhattal, S. J. Chapman, M. J. Disney, J. A.. Turner, Mon. Not. RAS **268**, 291 (1994)
21. J. E. Dale, I. A. Bonnell, A.. P. Whitworth, Mon. Not. RAS **375**, 1291 (2007)
22. N. Panagia, Astron. J. **78**, 929 (1973)
23. L. Zhu, Y.-F. Wu and Y. Wei, Chin. J. Astron. and Astrophys. **6**, 61 (2006)
24. L. Spitzer *Physical processes in the interstellar medium* (Wiley, New York, 1978; Mir, Moscow, 1981).
25. T. G. Bisbas, R. Wünsch, A.. P. Whitworth, D. A. Hubber, S. Walch, Astrophys. J., **736**, 142 (2011)
26. B. Lefloch, B. Lazareff, Astron. and Astrophys. **289**, 559 (1994)
27. P. F. Hopkins, Astrophys. J., **797**, 59 (2014)

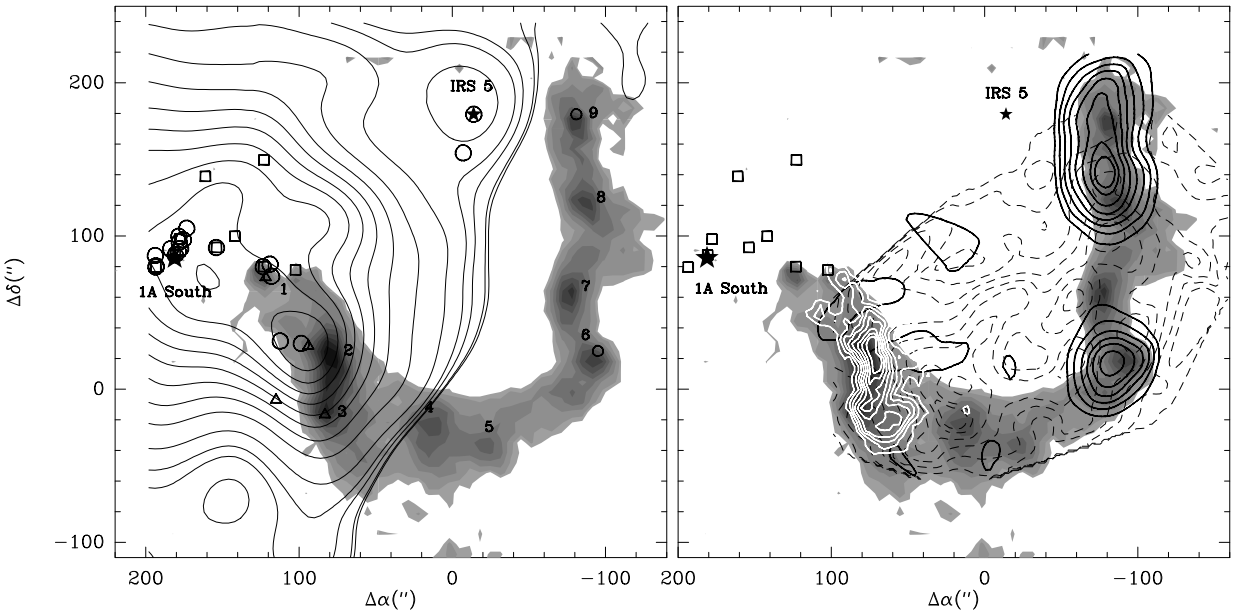

Figure 1. Maps of dust, ionized and molecular gas emission in the W40 region according to the data from [12]. The coordinates of the central position (the ^{13}CO emission peak [23]) are: R.A.(J2000)=$18^h\ 31^m\ 15.75^s$, Dec.(J2000)=–02° 06′ 49.3″. The clumpy ring is shown in greyscale. Distinct clumps are denoted by numbers (left panel). The spatial distribution of the ionized gas is shown as contours in the left panel. The HCN(1–0) (dashed contours), NH_3(1,1) (dark contours) and CS(5–4) (light contours) molecular line maps are shown in the right panel. Near IR-sources are shown as small squares [5]. Compact VLA radio sources [9] are shown as larger circles in the left panel. Class 0 and Class I sources [11] are marked by smaller circles and triangles, respectively (left panel). The driving source of the main HII zone, IRS 1A South, and the source of the separate H II zone, IRS 5, [5] are shown as stars.

Table 1. Observed and model parameters of the clumps

Parameter	Observed value	Model values	
	[12]	$L(photons/s) = 3 \cdot 10^{45}$	$L(photons/s) = 3 \cdot 10^{46}$
$n(\mathrm{cm}^{-3})$		10^5	$1.5 \cdot 10^5$
t_{dyn} (Myr)		0.65	0.45
t_{frag} (Myr)		0.44	0.3
R_{frag} (pc)	~ 0.3	0.24	0.23
$N_{frag}(10^{22}\ \mathrm{cm}^{-2})$	4–11	2.4	3.6
$M_{frag}(M_\odot)$	2–6	9.8	6.6
$2r_{frag}$ (pc)	$\sim 0.1 - 0.2$	0.27	0.18